Synthesis, Structure, and Reactivity of Homoleptic Tin(II) and Lead(II) Chalcogenolates and Their Conversion to Metal Chalcogenides. X-ray Crystal Structures of $\{Sn[TeSi(SiMe_3)_3]_2\}_2$ and $(PMe_3)Sn[TeSi(SiMe_3)_3]_2$

Allen L. Seligson and John Arnold*

Contribution from the Department of Chemistry, University of California, Berkeley, California 94720

Received April 8, 1993®

Abstract: The preparation and characterization of homoleptic tin(II) and lead(II) tellurolates, selenolates, and thiolates incorporating bulky $ESi(SiMe_3)_3$ ligands (E = Te, Se, S) are described. The derivatives $M[ESi(SiMe_3)_3]_2$ (M = Sn: **1**, E = Te; **3**, E = Se; **5**, E = S. M = Pb: **2**, E = Te; **4**, E = Se; **6**, E = S) are prepared via protonolysis of $M[N(SiMe_3)_2]_2$ with $HESi(SiMe_3)_3$. X-ray diffraction shows **1** to be dimeric in the solid state; it crystallizes in the space group $P2/c$ with a = 14.536(2) Å, b = 9.310(1) Å, c = 29.605(6) Å, β = 97.72(1)°, V = 3970.2(19) Å^3, Z = 4, R = 3.73%, and R_w = 3.85%. Reaction of **1** with PMe_3 affords the monomeric tin tellurolate $(PMe_3)Sn[TeSi(SiMe_3)_3]_2$ (**10**), while addition of 1 equiv of dmpe [dmpe = 1,2-bis(dimethylphosphino)ethane] to **1**, **3**, and **5** yields the dmpe-bridged stannyl chalcogenolates $\{Sn[TeSi(SiMe_3)_3]_2\}_2$(dmpe) (**7**, E = Te; **8**, E = Se; **9**, E = S). Complex **10** crystallizes in the space group $P\bar{1}$ with a = 9.625(1) Å, b = 14.236(3) Å, c = 16.973(4) Å, α = 100.59(2)°, β = 103.95(2)°, γ = 91.48(1)°, V = 2212.5(16) Å^3, Z = 2, R = 3.56%, and R_w = 4.52%. Pyrolysis of **1**, **2**, and **4** at relatively low temperatures (ca. 250 °C) under N_2 affords the cubic solids SnTe, PbTe, and PbSe and a single byproduct $E[Si(SiMe_3)_3]_2$ (E = Te, Se). The composition and crystallinity of these solids were confirmed by elemental analysis and X-ray powder diffraction. Related decomposition reactions also occur at even lower temperatures by thermolysis, UV irradiation, or addition of Lewis bases to hydrocarbon solutions.

Introduction

In general, homoleptic chalcogenolate complexes of coordinatively unsaturated metals tend to form oligomeric or polymeric networks as a result of bridging via lone pairs on the chalcogen.[1-3] Most compounds reported to date involve phenyl chalcogenolate ligands; they are often insoluble in common solvents and are, therefore, difficult to purify and characterize.[4,5] For alkoxides and thiolates, substitution at the ortho positions of the aryl ring or use of bulky alkyl groups increases the steric demand of the ligand to the point where low-molecularity species may be isolated. This methodology has been successful for the synthesis of several divalent group 14 metal alkoxides, siloxides, aryloxides, and thiolates.[6-15] We are interested[16,17] in developing the chemistry of complexes involving heavier chalcogenolate ligands (tellurolates and selenolates) and now present our findings on the chemistry of the first such derivatives of divalent Sn and Pb.

Applications of binary and ternary group 14 metal sulfides, selenides, and tellurides include the generation, transmission, or detection of electromagnetic radiation.[18] Present technology for the preparation of the group 14 metal chalcogenides includes precipitation from aqueous solution,[19,20] deposition from the gas phase (OMVPE),[21] or reaction of the elements at elevated temperatures.[22] More recently, the pyrolysis of $(Ph_2SnE)_3$ (E = S, Se) ring compounds yielded crystalline SnS and SnSe.[23]

The interest in chalcogenolate compounds as single-source precursors for metal chalcogenides[24] has been tempered by our limited knowledge of their molecular chemistry. Our recent efforts have led to the development of a series of new sterically demanding tellurolate, selenolate, and thiolate ligands based on the bulky silyl substituent $-Si(SiMe_3)_3$.[25-32] We have demonstrated the versatility of these ligands by the formation of stable, well-defined

* Abstract published in *Advance ACS Abstracts*, August 15, 1993.

(1) Craig, D.; Dance, I. G.; Garbutt, R. *Angew. Chem., Int. Ed. Engl.* **1986**, *25*, 165.
(2) Dance, I. G. *Polyhedron* **1986**, *5*, 1037.
(3) Gysling, H. J. In *The Chemistry of Organic Selenium and Tellurium Compounds*; Patai, S., Rappoport, Z., Eds.; Wiley: New York, 1986; Vol. 1, p 679.
(4) Gysling, H. J. *Coord. Chem. Rev.* **1982**, *42*, 133.
(5) Okamota, Y.; Yano, T. *J. Organomet. Chem.* **1971**, *29*, 99.
(6) Hitchcock, P. B.; Lappert, M. F.; Samways, B. J.; Weinberg, E. L. *J. Chem. Soc., Chem. Commun.* **1983**, 1492.
(7) Hitchcock, P. B.; Jasim, H. A.; Kelly, R. E.; Lappert, M. F. *J. Chem. Soc., Chem. Commun.* **1985**, 1776.
(8) Cetinkaya, B.; Gümrükcü, I.; Lappert, M. F.; Atwood, J. L.; Rogers, R. D.; Zaworotko, M. J. *J. Am. Chem. Soc.* **1980**, *102*, 2088.
(9) Fjeldberg, T.; Hitchcock, P. B.; Lappert, M. F.; Smith, S. J.; Thorne, A. J. *J. Chem. Soc., Chem. Commun.* **1985**, 939.
(10) du Mont, W.-W.; Grenz, M. *Z. Naturforsch., B* **1983**, *38B*, 113.
(11) Grenz, M.; Hahn, E.; du Mont, W.-W.; Pickardt, J. *Angew. Chem., Int. Ed. Engl.* **1984**, *23*, 61.
(12) Silverman, L. D.; Zeldin, M. *Inorg. Chem.* **1980**, *19*, 270.
(13) du Mont, W.-W.; Grenz, M. *Chem. Ber.* **1981**, *114*, 1180.
(14) Veith, M.; Recktenwald, O. *Top. Curr. Chem.* **1982**, *104*, 1.
(15) Veith, M. *Chem. Rev.* **1990**, *90*, 3.
(16) Bonasia, P. J.; Arnold, J. *J. Organomet. Chem.* **1993**, *449*, 147.
(17) Bonasia, P. J.; Arnold, J. *J. Chem. Soc., Chem. Commun.* **1990**, 1299.
(18) Strauss, A. J. In *Concise Encyclopedia of Semiconducting Materials and Related Technologies*; Mahajan, S., Kimerling, L. C., Ed.; Pergamon: New York, 1992; p 427.
(19) Putley, E. H. *Lead Sulfide, Selenide and Telluride*; Wiley: New York, 1965.
(20) Korczynski, A.; Lubomirska, I.; Sobierajski, T. *Chem. Stosow.* **1981**, *25*, 391.
(21) Manasevit. H. M.; Simpson, W. I. *J. Electrochem. Soc.* **1975**, *122*, 444.
(22) Yellin, N.; Ben-Dor, L. *Mater. Res. Bull.* **1983**, *18*, 823.
(23) Bahr, S. R.; Boudjouk, P.; McCarthy, G. J. *Chem. Mater.* **1992**, *4*, 383.
(24) O'Brien, P. *Chemtronics* **1991**, *5*, 61.
(25) Bonasia, P. J.; Gindelberger, D. E.; Dabbousi, B. O.; Arnold, J. *J. Am. Chem. Soc.* **1992**, *114*, 5209.
(26) Bonasia, P. J.; Arnold, J. *Inorg. Chem.* **1992**, *31*, 2508.
(27) Christou, V.; Arnold, J. *J. Am. Chem. Soc.* **1992**, *114*, 6240.
(28) Gindelberger, D. E.; Arnold, J. *J. Am. Chem. Soc.* **1992**, *114*, 6242.
(29) Arnold, J.; Walker, J. M.; Yu, K. M.; Bonasia, P. J.; Seligson, A. L.; Bourret, E. D. *J. Cryst. Growth* **1992**, *124*, 674.
(30) Seligson, A. L.; Bonasia, P. J.; Arnold, J.; Yu, K. M.; Walker, J. M.; Bourret, E. D. *Mater. Res. Soc. Symp. Proc.* **1992**, *282*, 665.
(31) Cary, D. R.; Arnold, J. *J. Am. Chem. Soc.* **1993**, *115*, 2520.
(32) Bonasia, P. J.; Christou, V.; Arnold, J. *J. Am. Chem. Soc.*, in press.

0002-7863/93/1515-8214$04.00/0

metal complexes of low molecularity and increased hydrocarbon solubility.[33] Here, the ubiquity of $-ESi(SiMe_3)_3$ (E = Te, Se, S) ligands is extended to complexes of the divalent group 14 metals tin and lead. This paper focuses on the synthesis and characterization of these molecules and their conversion to crystalline tin and lead chalcogenides.

Results and Discussion

Homoleptic Chalcogenolates. The protonolysis reactions between $HESi(SiMe_3)_3$ (E = Te, Se, S) and group 14 divalent amides in hydrocarbon solvents provide high-yield synthetic routes to homoleptic tellurolates, selenolates, and thiolates of Sn(II) and Pb(II) (eq 1). Alternatively, **1** can be synthesized by the

$$2HESi(SiMe_3)_3 + M[N(SiMe_3)_2]_2 \rightarrow M[ESi(SiMe_3)_3]_2 + 2HN(SiMe)_3 \quad (1)$$
1–6

M = Sn: **1**, E = Te; **3**, E = Se; **5**, E = S

M = Pb: **2**, E = Te; **4**, E = Se; **6**, E = S

metathesis reaction between 2 equiv of $(THF)_2LiTeSi(SiMe_3)_3$ and $SnCl_2$ in hexane, but the yield is much lower. For the lead derivative **2**, tellurolysis is the only successful approach as interaction of $(THF)_2LiTeSi(SiMe_3)_3$ with $PbCl_2$ in hexane yields only Pb(0) and $Te_2[Si(SiMe_3)_3]_2$. Complexes **1–4** are the first examples of tellurolates and selenolates for Sn(II) and Pb(II).

The homoleptic compounds **1–6** are bright red or orange materials that can be crystallized from concentrated hexane or pentane in high yields. They are stable for prolonged periods under nitrogen at room temperature; however, they decompose slowly when exposed to air to form the dichalcogenides $E_2[Si(SiMe_3)_3]_2$ (E = Te, Se, S).

In the EI mass spectra of **3** and **5**, the highest mass peaks corresponded to the monomeric species $M[ESi(SiMe_3)_3]_2$ (M = Sn; E = Se, S) with fragmentation peaks at lower mass due to $E[Si(SiMe_3)_3]_2$ and $E_2[Si(SiMe_3)_3]_2$. For the tellurolates, no molecular ions were detected and only signals due to $Te[Si(SiMe_3)_3]_2$ and $Te_2[Si(SiMe_3)_3]_2$ were observed.

Room-temperature ^1H NMR spectra of **1–6** in toluene-d_8 display sharp singlets at similar chemical shifts. At the same temperature, the $^{13}C\{^1H\}$ NMR signals are slightly more sensitive to substitution and a small upfield shift is observed upon moving from Te to S. This trend is similar to that observed for $HESi(SiMe_3)_3$ (E = Te, Se, S).[32] Unfortunately, all attempts to observe ^{119}Sn, ^{125}Te, and ^{77}Se NMR signals were in vain, even down to low temperatures (–75 °C).

The singlet in the ^1H NMR spectrum of **2** broadens and shifts slightly on cooling. By –70 °C this broad peak (0.44 ppm) is accompanied by a new broad resonance at 0.38 ppm. The intensity of this new resonance increases on further cooling, but even at our low-temperature limit (–90 °C) the downfield peak is still 2.5 times as intense as the new upfield resonance. NMR data for compound **1** are essentially identical, but for the tin selenolate complex **3**, the two singlets are present in a 4:1 ratio at –90 °C. Raising the temperature had no effect on the spectra of **1** and **2**, which were invariant up to 100 °C. In contrast, variable-temperature ^1H NMR studies on the selenolate **4** and thiolates **5** and **6** showed no evidence for splitting or decoalesence over a temperature range from –90 to 100 °C.

The presence of inequivalent resonances in the low-temperature ^1H NMR spectra of **1–3** may result from either monomer/oligomer equilibria or *cis*/*trans* isomerization of a dimeric species such as that shown Monomeric, dimeric, and trimeric units of

A B

several group 14 alkoxides and thiolates have been characterized in the solid state and gas phase.[6-9,11,14,15] In these derivatives, oligomerization is clearly related to the steric bulk of the alkyl or aryl group bound to oxygen or sulfur. Although tellurolate and selenolate ligands are notoriously good bridging ligands,[1-5] the bulky $ESi(SiMe_3)_3$ (E = Te, Se, S) ligands are known to inhibit this tendency in related metal complexes.[26-28,30,31] The second explanation assumes that lone pairs of electrons on the metal centers are stereochemically active, such that the two monomeric units of the dimer can orient themselves with the lone pairs positioned on either the same side [*cis* (**A**)] or opposite sides [*trans* (**B**)] of the dimer. This type of behavior has been observed in both solution and the solid state for homoleptic group 14 and 15 phosphide complexes.[34-37] Theoretical calculations on the model complexes M_2H_4 (M = Sn, Pb) suggest that the *cis* and *trans* forms of the dimer are approximately isoenergetic.[38] The observance of only one isomer of the dimer in solution at room temperature may result from the increased steric demands of the $-ESi(SiMe_3)_3$ (E = Te, Se, S) ligands.

Although the exact solution structures of these compounds are presently uncertain, the solid-state structure of **1** is clearly dimeric as shown by X-ray crystallography (see Figure 1). Pertinent bond lengths and angles are listed in Table II. The compound crystallizes in the space group $P2/c$ with a crystallographic 2-fold axis relating the two Sn atoms and the bridging and terminal tellurolate ligands. The Sn_2Te_2 core of the dimer is butterflied with an acute Te1–Sn–Te1 angle [78.71(2)°] and a slightly obtuse Sn–Te1–Sn angle [91.65(2)°]. Only the *cis* isomer is observed, with both lone pairs of electrons on the metal centers residing on the same side of the complex (cf. structure **A**). The presence of the lone pair therefore results in a structure that is quite different from that of the related zinc complex $\{Zn[TeSi(SiMe_3)_3]_2\}_2$, in which the terminal tellurolates adopt a *trans* arrangement across a fairly planar M_2Te_2 core.[26] Consideration of the angles about Sn [Te1–Sn–Te1 = 78.71(2)°; Te1–Sn–Te2 = 84.28(2), 94.25(3)°] suggests a high degree of p character in these bonds. It has been proposed that lower degrees of hybridization are favored in heavier metals such as Sn(II) where the nonbonding pair of electrons possesses increased s orbital character.[15,39,40] The roughly equivalent Sn–Te1 bond lengths [2.946(1), 2.956(1) Å] suggest a high degree of delocalization in the Sn_2Te_2 core. As expected, the bond lengths to the bridging ligands are considerably longer than the Sn–Te2 terminal bond distance of 2.800(1) Å (analogous trends have been observed in group 14 thiolate and alkoxide complexes[6-9,14,15]). The bridging Sn–Te bond lengths are also longer than the Sn–Te distances in known cyclic $Sn_2(\mu_2\text{–}Te)_2$ complexes by approximately 0.1–0.2 Å.[41,42]

Gas-phase diffraction of the *trans* isomer of $[Sn(O^tBu)_2]_2$ shows the complex contains a planar Sn_2O_2 core with an acute O_b–

(33) For related work on derivatives of this ligand see: Becker, G.; Klinkhammer, K. W.; Lartiges, S.; Bottcher, P.; Poll, W. *Z. Anorg. Allg. Chem.* **1992**, *613*, 7. Uhl, W.; Layh, M.; Becker, G.; Klinkhammer, K. W.; Hildenbrand, T. *Chem. Ber.* **1992**, *125*, 1547. Becker, G.; Klinkhammer, K. W.; Schwarz, W.; Westerhausen, M.; Hildenbrand, T. *Z. Naturforsch., B* **1992**, *47B*, 1225.

(34) Jutzi, P.; Meyer, U.; Opelia, S.; Olmstead, M. M.; Power, P. P. *Organometallics* **1990**, *9*, 1459.
(35) Goel, S. C.; Chiang, M. Y.; Rauscher, D. J.; Buhro, W. E. *J. Am. Chem. Soc.* **1993**, *115*, 160.
(36) Cowley, A. H.; Giolando, D. M.; Jones, R. A.; Nunn, C. M.; Power, J. M. *Polyhedron* **1988**, *7*, 1909.
(37) du Mont, W.-W.; Kroth, H.-J. *Angew. Chem., Int. Ed. Engl.* **1977**, *16*, 792.
(38) Trinquier, G. *J. Am. Chem. Soc.* **1990**, *112*, 2130.
(39) Kaupp, M.; Schleyer, P. v. R. *J. Am. Chem. Soc.* **1993**, *115*, 1601.
(40) Kutzelinigg, W. *THEOCHEM* **1988**, *169*, 403.
(41) Hitchcock, P. B.; Jasim, H. A.; Lappert, M. F.; Leung, W.-P.; Rai, A. K.; Taylor, R. E. *Polyhedron* **1991**, *10*, 1203.
(42) Puff, H.; Bertram, G.; Ebeling, B.; Franken, M.; Gattermayer, R.; Hundt, R.; Schuh, W.; Zimmer, R. *J. Organomet. Chem.* **1989**, *379*, 235.

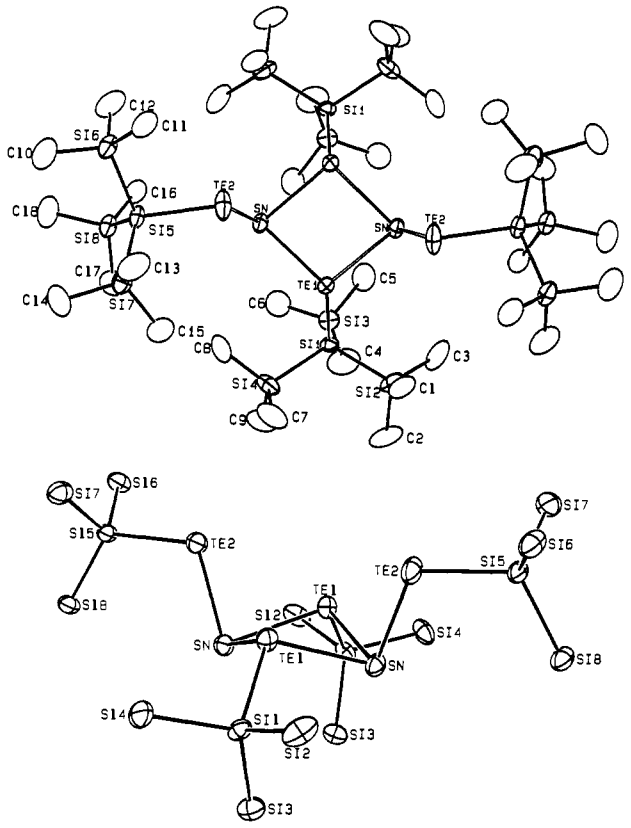

Figure 1. Top: ORTEP view of the molecular structure of **1**. Bottom: ORTEP view of **1** emphasizing the "butterflied" Sn_2Te_2 core (methyl groups omitted for clarity).

Table I. Crystallographic Parameters for **1** and **10**

	1	**10**
formula	$SnTe_2Si_8C_{18}H_{54}$	$SnTe_2Si_8PC_{21}H_{63}$
mol wt	869.2	945.3
crystal size, mm	0.11 × 0.22 × 0.18	0.24 × 0.31 × 0.34
space group	$P2/c$	$P\bar{1}$
a, Å	14.536(2)	9.625(1)
b, Å	9.310(1)	14.236(3)
c, Å	29.605(6)	16.973(4)
α, deg	90.0	100.59(2)
β, deg	97.72(1)	103.95(2)
γ, deg	90.0	91.48(1)
V, Å^3	3970.2(19)	2212.5(16)
Z	4	2
d_{calcd}, g cm^{-3}	1.45	1.42
radiation; λ, Å	Mo Kα; 0.710 73	Mo Kα; 0.710 73
scan mode	ω	θ–2θ
2θ range, deg	3–45	3–45
collection range	$+h,+k,\pm l$	$+h,\pm k,\pm l$
scan speed, deg/min	5.49	5.49
abs coeff (μ), cm^{-1}	23.4	21.4
no. of reflns coll	5784	5782
no. of unique reflns	5171	5782
no. of reflns with $F^2 > 3\sigma(F^2)$	3502	4927
final R, R_w	0.0373, 0.0385	0.0356, 0.0452
T, °C	−130	−91

Sn–O_b angle of 76(2)°.[9] The stereochemical activity of the lone pairs on these Sn(II) centers indicates a significant degree of p character in the orbital rather than pure s character, as the inert-pair effect might suggest.[15,39,40,43] In fact, reports of Sn(II) compounds containing *non*stereochemically active lone pairs are extremely rare.[14]

Donor Complexes. Lewis acids such as BF_3, $Cr(CO)_5$, and "Cp_2Zr" are reported to form stable adducts with several Sn(II) complexes;[14,44–51] however, we found no evidence for such adduct formation with any of the homoleptic chalcogenolates **1–6**. Considering the dimeric structure of **1** to involve donation of a lone pair of electrons on Te to a vacant orbital on Sn suggested that Lewis base adducts might afford monomeric derivatives. Thus, addition of PMe_3 to a hexane solution of **1** yielded orange crystals of the Lewis acid–base adduct **10** (eq 2). The coordination

$$\{Sn[TeSi(SiMe_3)_3]_2\}_2 + PMe_3 \rightarrow (PMe_3)Sn[TeSi(SiMe_3)_3]_2 \quad (2)$$

of PMe_3 is confirmed by the appearance of a singlet in the $^{31}P\{^1H\}$ NMR spectrum flanked by $^{117/119}Sn$ satellites. The $^{31}P\{^1H\}$ NMR resonance (−78.9 ppm) is shielded slightly compared to that of free PMe_3 (−62 ppm). The value of $|J_{^{31}P^{117/119}Sn}|$ (1580 Hz) is greater than that in related Sn(II) compounds[52] such as $Sn(SCH_2CH_2)_2PPh$,[53] where the coupling constant is 1244 Hz. A doublet flanked by $^{117/119}Sn$ satellites is seen in the ^{125}Te NMR spectrum (−1165 ppm, $|^2J_{TeP}| = 79$ Hz; $|J_{Te^{117/119}Sn}| = 1327$ Hz). The magnitude of $J_{Te^{117/119}Sn}$ is considerably smaller than those reported for Sn(IV) complexes with bridging telluride ligands that fall in the range 1900–2700 Hz.[41,42,54]

Table II. Selected Bond Distances (Å) and Angles (deg) for **1**

Sn–Te1	2.956(1)	Sn–Te1	2.946(1)
Sn–Te2	2.800(1)	Te1–Si1	2.540(2)
Te2–Si5	2.521(2)	Si1–Si2	2.344(4)
Si1–Si3	2.348(4)	Si1–Si4	2.336(3)
Si2–C1	1.854(11)	Si2–C2	1.878(11)
Si2–C3	1.851(11)	Te1–Sn–Te1	78.71(2)
Te1–Sn–Te2	94.25(3)	Te1–Sn–Te2	84.28(2)
Sn–Te1–Sn	91.65(2)	Sn–Te1–Si1	108.67(6)
Sn1–Te1–Si1	102.76(6)	Sn–Te2–Si5	111.68(6)
Te1–Si1–Si2	102.91(12)	Te1–Si1–Si3	114.55(11)
Te1–Si1–Si4	102.26(11)	Si2–Si1–Si3	113.45(13)
Si2–Si1–Si4	111.89(14)	Si3–Si1–Si4	111.03(14)

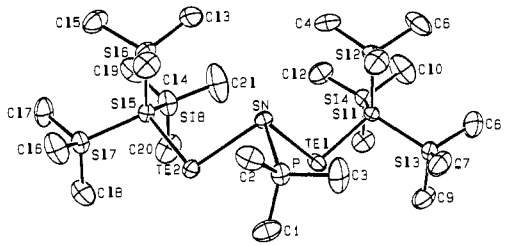

Figure 2. ORTEP view of the molecular structure of **10**.

X-ray crystallography confirmed the structure of **10** as that shown in Figure 2. Relevant bond lengths and angles are given in Table III. The ligands are arranged in a trigonal-pyramidal geometry with the lone pair presumably occupying the remaining coordination site. As in the dimer **1**, the angles about Sn also approach 90° but the Te1–Sn–Te2 bond angle [98.86(2°)] is slightly larger than the corresponding angle in the former. Taken

(43) Huheey, J. E. *Inorganic Chemistry*, 3rd ed.; Harper and Row: New York, 1983.
(44) Hsu, C. C.; Geanangel, R. A. *Inorg. Chim. Acta* **1979**, *34*, 241.
(45) Hsu, C. C.; Geanangel, R. A. *Inorg. Chem.* **1980**, *19*, 110.
(46) Harrison, P. G.; Zuckerman, J. J. *J. Am. Chem. Soc.* **1970**, *92*, 2577.
(47) Cornwell, A. B.; Harrison, P. G.; Richards, J. A. *J. Organomet. Chem.* **1972**, *108*, 47.
(48) Cotton, J. D.; Davidson, P. J.; Lappert, M. F. *J. Chem. Soc., Dalton Trans.* **1976**, 2275.
(49) Lappert, M. F.; Power, P. P. *Adv. Chem. Ser.* **1976**, *157*, 70.
(50) Piers, W. E.; Whittal, R. M.; Ferguson, G.; Froese, R. D. J.; Stronks, H. J.; Krygsman, P. H. *Organometallics* **1992**, *11*, 4015.
(51) Cotton, J. D.; Davison, P. J.; Goldberg, D. E.; Lappert, M. F.; Thomas, K. M. *J. Chem. Soc., Chem. Commun.* **1974**, 893.
(52) Kennedy, J. D.; McFarlane, W. In *Multinuclear NMR*; Mason, J., Ed.; Plenum Publishing Corp.: New York, 1987; p 305.
(53) Baumeister, U.; Hartung, H.; Jurkschat, K.; Tzschach, A. *J. Organomet. Chem.* **1986**, *304*, 107.
(54) Schäfer, A.; Weidenbruch, M.; Saak, W.; Pohl, S.; Marsmann, H. *Angew. Chem., Int. Ed. Engl.* **1991**, *30*, 834.

Table III. Selected Bond Distances (Å) and Angles (deg) for **10**

Sn–Te1	2.834(1)	Sn–Te2	2.843(1)
Sn–P	2.663(2)	Te1–Si1	2.531(1)
Te2–Si5	2.522(2)	P–C1	1.800(7)
P–C2	1.806(7)	P–C3	1.805(7)
Si1–Si2	2.351(2)	Si1–Si3	2.348(2)
Si1–Si4	2.346(2)	Si2–C4	1.862(7)
Si2–C5	1.877(7)	Si2–C6	1.872(7)
Te1–Sn–Te2	98.86(2)	Te1–Sn–P	90.24(4)
Te2–Sn–P	84.83(4)	Sn–Te1–Si1	102.08(4)
Sn–Te2–Si5	97.61(4)	Sn–P–C1	117.8(2)
Sn–P–C2	109.3(2)	Sn–P–C3	114.3(2)
Te–Si1–Si2	116.26(7)	Te–Si1–Si3	103.03(7)
Te–Si1–Si4	105.41(7)	Si2–Si1–Si3	110.85(8)
Si2–Si1–Si4	110.51(9)	Si3–Si1–Si4	110.42(9)
Si1–Si2–C4	110.8(2)	Si1–Si2–C5	113.0(2)
Si1–Si2–C6	109.0(2)		

Table IV. ^{31}P NMR Data for $(PR_3)Sn[TeSi(SiMe_3)_3]_2$

PR_3	$\delta(^{31}P\{^1H\})$	$J_{P117/119Sn}$, Hz[a]	$\Delta\delta(^{31}P\{^1H\})$[b]	cone angle, deg[c]	pK_b[d]
PMe_3	−79	1580	17	118	8.65
PMe_2Ph	−71	1512	25	122	6.49
PEt_3	−42	1640	23	132	8.69
PCy_3	−22	1777	29	170	9.70
dmpe	−60	1555	10	107	8.62[e]
PPh_3	−11		0	145	2.73
$P(OMe)_3$	136		0	107	

[a] Taken from $^{31}P\{^1H\}$ NMR spectrum. [b] $\Delta\delta(^{31}P) = \delta(^{31}P_{complex}) - \delta(^{31}P_{ligand})$. [c] Values taken from: Tolman, C. A. *Chem. Rev.* **1977**, *77*, 313. [d] Values taken from: Henderson, W. M., Jr.; Streuli, C. A. *J. Am. Chem. Soc.* **1960**, *82*, 5791. [e] pK_b estimated to.be the same as that for PMe_2Et.

together with the rather acute Te1–Sn–P angles [90.24(4), 84.83(4)°], these data suggest that the steric bulk of the tellurolate ligands plays a significant role in determining the structure. The Sn–Te bond distances [2.834(1), 2.843(1) Å] are slightly longer than the terminal Sn–Te bonds in the structure of **1**. The Sn–P bond distance [2.663(2)°] and the angles around the Sn center are comparable to those in $Sn(SCH_2CH_2)_2PPh$.[53]

$^{31}P\{^1H\}$ NMR data for a range of phosphine adducts analogous to **10** are listed in Table IV. Complexation of the ligand results in an upfield shift of the $^{31}P\{^1H\}$ resonance in all cases. Values of $|J_{P117/119Sn}|$ appear to increase relative to the basicity of the phosphine.[55] Steric hindrance (as gauged by cone angles[56]) correlates well with the coordination shift factor $\Delta\delta(^{31}P)$ $(=|\delta(^{31}P_{complex}) - \delta(^{31}P_{ligand})|)$ for the limited number of phosphines studied. Weak bases, such as PPh_3 and $P(OMe)_3$, do not form observable complexes with **1**, suggesting that the basicity of the phosphine, rather than its steric bulk, is more important in determining stability. Related Lewis base adducts of Sn(II) halides were described a number of years ago by du Mont and co-workers.[57,58]

Addition of 1 equiv of the chelating phosphine dmpe to a hexane solution of **1** resulted in the precipitation of complex **7**. The $^{125}Te\{^1H\}$ NMR spectrum of **7** at −70 °C consists of a doublet at −1175 ppm; the similarity of the tin–phosphorus coupling constant ($|^2J_{Te^{31}P}| = 64$ Hz) to that in **10** implies the structure shown in eq 3. The $^{31}P\{^1H\}$ NMR spectrum shows a singlet at −60.4 ppm flanked by $^{117/119}Sn$ satellites with $|J_{P117/119Sn}| = 1555$ Hz. The analogous selenolate and thiolate complexes **8** and **9** were also prepared, and they show similar spectroscopic and physical characteristics. Comparison of the room-temperature $^{31}P\{^1H\}$ NMR chemical shifts of complexes **7**–**9** (−60.4, −47.2, and −35.4 ppm, respectively) reveals a downfield shift upon going

$$2\{Sn[TeSi(SiMe_3)_3]_2\}_2 + dmpe \longrightarrow$$

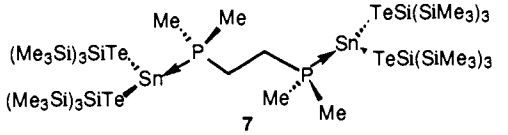

7 (3)

from tellurium to sulfur, while the phosphorus–tin coupling constants are quite invariant. This implies that although the phosphorus becomes less shielded by a tin center bound to chalcogen atoms of increased electronegativity, there is little change in the s orbital character of the P–Sn(II) bond.

Molecule to Solid-State Conversions. Pyrolyses of **1**–**6** were conducted in quartz tubes under a slow stream of N_2 at atmospheric pressure. Complexes **1**, **2**, and **4** decompose cleanly at 250 °C according to eq 4. For each reaction, both products

$$M[ESi(SiMe_3)_3]_2 \rightarrow (ME)_n + E[Si(SiMe_3)_3]_2 \quad (4)$$

$$M = Sn\ (E = Te),\ Pb\ (E = Te, Se)$$

were isolated and characterized: the metal chalcogenides were recovered as metallic gray powders, and the corresponding disilyl chalcogenides, which condensed at the cold end of the tube, were isolated as waxy yellow or colorless films. The metal chalcogenides are relatively pure; however, they always contain small amounts of carbon and hydrogen (they were not analyzed for silicon) as shown in Table V. Pyrolysis of complexes **3**, **5**, and **6** under similar conditions also yielded metallic powders, but these proved to be extremely rich in elemental Pb or Sn metal and the $E[Si(SiMe_3)_3]_2$ (E = Se, S) byproducts were contaminated with unidentifiable $SiMe_3$-containing species.

The crystallinity of the metallic powders from pyrolysis of **1**, **2**, and **4** was verified by X-ray diffraction. The X-ray diffraction pattern of PbSe shown in Figure 3 and those of cubic SnTe and PbTe are in very good agreement with literature values given in Table VI. No extraneous peaks due to other phases of ME were observed, although the presence of small quantities of amorphous material was evident by the broad rolling baseline of the powder diffractions; this is consistent with the carbon and hydrogen impurities detected by elemental analysis. This route to group 14 chalcogenides occurs at temperatures below those of other previously reported preparations.[21,22] Diffraction patterns of the powders from pyrolysis of **3** and **6** indicated the presence of elemental Sn and Pb in addition to cubic ME [M = Sn (E = Se), Pb (E = S)].

Clean solid-state pyrolysis of compounds **1**, **2**, and **4** according to eq 4 parallels our earlier reports on both the gas-phase pyrolysis of $M[EX(SiMe_3)_3]_2$ (M = Zn, Cd, Hg; E = Te, Se; X = C, Si), yielding crystalline thin films of ME[29,30] and bulk pyrolyses of early transition metal and lanthanide tellurolates, which gave crystalline MTe phases.[27,31] These decomposition reactions are not unique to the tris(trimethylsilyl)silyl chalcogenolate ligands as bulk- and gas-phase pyrolysis of other metal chalcogenolate complexes has also been observed.[59–66] Boudjouk and co-workers studied the bulk pyrolysis of the group 14–16 compounds

(55) Henderson, W. A., Jr.; Streuli, C. A. *J. Am. Chem. Soc.* **1960**, *82*, 5791.
(56) Tolman, C. A. *Chem. Rev.* **1977**, *77*, 313.
(57) du Mont, W.-W.; Neudert, B.; Rudolph, G.; Schumann, H. *Angew. Chem., Int. Ed. Engl.* **1976**, *15*, 308.
(58) du Mont, W.-W.; Neudert, B. *Z. Anorg. Allg. Chem.* **1978**, *441*, 86.
(59) Steigerwald, M. L.; Sprinkle, C. R. *J. Am. Chem. Soc.* **1987**, *109*, 7200.
(60) Brennan, J. G.; Siegrist, T.; Carroll, P. J.; Stuczynski, S. M.; Reynders, P.; Brus, L. E.; Steigerwald, M. L. *Chem. Mater.* **1990**, *2*, 403.
(61) Strzelecki, A. R.; Timinski, P. A.; Helsel, B. A.; Bianconi, P. A. *J. Am. Chem. Soc.* **1992**, *114*, 3159.
(62) Bochmann, M.; Webb, K. J.; Hails, J. E.; Wolverson, D. *Eur. J. Solid State Inorg. Chem.* **1992**, *29*, 155.
(63) Bochmann, M.; Webb, K.; Harman, M.; Hursthouse, M. B. *Angew. Chem., Int. Ed. Engl.* **1990**, *29*, 638.
(64) Bochmann, M.; Webb, K. J.; Hursthouse, M. B.; Mazid, M. *J. Chem. Soc., Dalton Trans.* **1991**, 2317.
(65) Brennan, J. G.; Siegrist, T.; Carroll, P. J.; Stuczynski, S. M.; Brus, L. E.; Steigerwald, M. L. *J. Am. Chem. Soc.* **1989**, *111*, 4141.
(66) Stuczinski, S. M.; Brennan, J. G.; Steigerwald, M. L. *Inorg. Chem.* **1989**, *28*, 4431.

Table V. Atomic Adsorption and Combustion Analyses for ME Powders from the Solid-State Pyrolysis of $M[ESi(SiMe_3)_3]_2$[a]

compd pyrolyzed	ME	wt % of powder recovered[c]	wt %[b] M	E	C	H
1	SnTe	28 (28)	46.2 (48.19)	39.7 (51.81)	3.05	0.74
2	PbTe	31 (35)	55.5 (61.89)	38.3 (38.11)	0.52	0.14
4	PbSe	32 (33)	62.2 (72.41)	23.5 (27.59)	1.86	0.41

[a] The powders from the pyrolysis of compounds **3**, **5**, and **6** were determined to contain elemental Sn and Pb impurities by X-ray diffraction studies. [b] Calculated weight percentage for ME in parentheses. [c] Theoretical percentage of ME recovered based on complete conversion of $M[ESi(SiMe_3)_3]_2$ to ME and $E[Si(SiMe_3)_3]_2$.

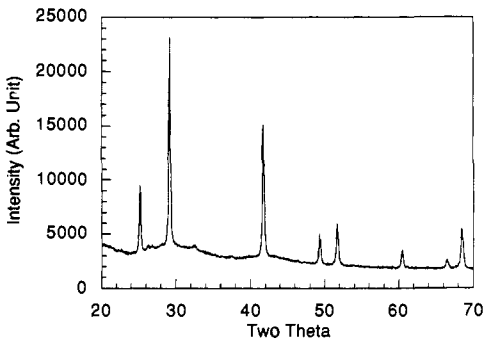

Figure 3. X-ray diffraction pattern of PbSe from the pyrolysis of **4** at 250 °C.

Table VI. X-ray Powder Diffraction Data

	experimental: solid-state pyrolysis		experimental: soln thermolysis[b]		standards[a]		
ME	*d* (Å)	intens	*d* (Å)	intens	*d* (Å)	*hkl*	intens
SnTe	3.1594	s	3.1755	s	3.15	200	s
	2.2327	s	2.2423	s	2.23	220	s
	1.8232	m	1.8305	m	1.822	222	w
	1.5791	w	1.5832	w	1.577	400	w
	1.4127	w	1.4169	w	1.410	420	w
	1.2886	w	1.2392	w	1.287	422	w
PbTe	3.7345	m	3.7300	m	3.7319	111	w
	3.2306	s	3.2302	s	3.2325	200	s
	2.2842	s	2.2837	m	2.2845	220	s
	1.9481	w	1.9476	w	1.9481	311	w
	1.8645	m	1.8652	m	1.8650	222	m
	1.6149	w	1.6137	w	1.6151	400	w
	1.4443	w	1.4443	w	1.4447	420	w
	1.3184	w	1.3186	w	1.3185	422	w
PbSe	3.5373	m	3.5339	m	3.536	111	m
	3.0627	s	3.0601	s	3.062	200	s
	2.1654	s	2.1642	s	2.165	220	s
	1.8466	w	1.8454	w	1.846	311	w
	1.7681	w	1.7674	w	1.768	222	w
	1.5310	w	1.5302	w	1.531	400	w
	1.3698	w	1.3691	w	1.369	420	w

[a] Cubic SnTe JCPDS No. 8-487, cubic PbTe JCPDS No. 38-1435, cubic PbSe JCPDS No. 6-354. [b] Small amounts of Sn metal (JCPDS No. 4-0673) were observed in the powder diffraction pattern of SnTe from solution thermolysis of **1**.

$(Ph_2SnE)_3$ (E = S, Se) which yielded crystalline ME solids.[23] It is worth noting that pyrolysis of the latter Sn(IV) complexes yielded only the orthohombic form of SnSe and, though the pyrolysis products of complex **3** were contaminated by Sn metal, cubic SnSe was the only phase identified by X-ray diffraction.

Thermolysis of $M[ESi(SiMe_3)_3]_2$ (M = Sn, Pb; E = Te, Se, S) complexes in aromatic hydrocarbon solvents also results in the formation of ME and $E[Si(SiMe_3)_3]_2$ according to eq 2. When a toluene solution of compound **2** was heated to 100 °C for 22 h, a gray metallic precipitate of PbTe was obtained. Elemental analysis (Table VII) and X-ray powder diffraction (Table VI) confirmed this to be cubic PbTe. The yellow supernatant contained only $Te[Si(SiMe_3)_3]_2$, and the overall mass recovery was 95%. Solution thermolysis of complexes **1** and **4** yielded SnTe and PbSe, respectively. Compounds **3**, **5**, and **6** gave metallic precipitates under similar conditions; however, these reactions were not clean.

In related systems, we have shown that $Zn[TeSi(SiMe_3)_3]_2$ undergoes the same thermolysis reaction in solution, yielding crystalline ZnTe and $Te[Si(SiMe_3)_3]_2$.[67] This reaction is not specific to the heavier chalcogenides, as $Pb(OSiPh_3)_2$ has been reported to undergo a similar reaction in refluxing ether resulting in lead oxo–siloxo complexes and elimination of hexaphenyldisiloxane.[68] Formation of crystalline metal chalcogenides under these mild conditions may prove to be a useful synthetic procedure.

The decomposition reaction shown in eq 2 appears to be a common decomposition pathway for $M[ESi(SiMe_3)_3]_2$ complexes. UV irradiation of **2** in aromatic hydrocarbon solvent also results in the clean formation of $Te[Si(SiMe_3)_3]_2$ and a gray metallic precipitate, presumed to be PbTe. Steigerwald has reported the similar photolytic decomposition of $Hg(TePh)_n$ to HgTe and $TePh_2$.[60] Photolysis of **1** also yields a gray metallic precipitate, although $Te[Si(SiMe_3)_3]_2$ is not the sole byproduct observed in the reaction solution. The presence of unidentified $SiMe_3$-containing species may be the result of radical reactions. The disproportionation reaction of SnX_2 complexes to Sn(III) radical species is well documented.[6,49,69,70]

In certain cases, addition of Lewis bases promotes the decomposition to metal chalcogenides. For example, addition of excess CH_3CN to an ether solution of **2** results in quantitative conversion to cubic PbTe and $Te[Si(SiMe_3)_3]_2$. A single equivalent of pyridine reacts much faster to form the same products. Similar decomposition reactions were observed for **7–10**, although they occur at much slower rates.

Experimental Section

All operations were carried out under dry nitrogen unless stated otherwise. The metal amides,[71,72] $HESi(SiMe_3)_3$ and $(THF)_2LiESi(SiMe_3)_3$,[25,32] were prepared by literature methods. ^1H and $^{13}C\{^1H\}$ NMR spectra were recorded in benzene-d_6 at 20 °C unless stated otherwise. $^{31}P\{^1H\}$ NMR spectra were recorded at 161.977 MHz, with chemical shifts relative to external 85% H_3PO_4 at 0 ppm. The $^{125}Te\{^1H\}$ NMR spectra were recorded at 94.580 MHz, referenced indirectly to neat Me_2Te at 0 ppm by direct reference to external $Te(OH)_6$ (1.74 M in D_2O, 20 °C) at 712 ppm. X-ray powder diffraction (XRD) patterns were recorded on ground samples pressed into a grooved Plexiglas holder using an automated Siemens diffractometer with Cu Kα radiation and standard data reduction software. Elemental and MS analyses were performed by the microanalytical and mass spectrometry laboratories of the College of Chemistry, University of California, Berkeley. FAB MS was carried out using cesium as the atom source, nitrobenzyl alcohol (NBA) as the matrix, and positive-ion detection.

$\{Sn[TeSi(SiMe_3)_3]_2\}_2$ (1). A solution of $HTeSi(SiMe_3)_3$ (0.51 g, 1.36 mmol) in hexane (15 mL) was added to a solution of $Sn[N(SiMe_3)_2]_2$ (0.30 g, 0.68 mmol) in the same solvent (15 mL), resulting in the formation of a dark orange solution. The mixture was stirred for 1 h and the solvent removed under reduced pressure. The dry orange powder was extracted with hexane (15 mL), and the solution was filtered, concentrated to 2.5 mL, and cooled to −40 °C for 24 h. Orange crystals of **1** (0.48 g, 81%) were isolated by filtration in three crops. Mp: 192–195 °C dec. ^1H NMR (400 MHz): δ 0.42 (s). $^{13}C\{^1H\}$ NMR (100 MHz): δ 2.42 (s). IR: 1259 w, 1243 m, 1019 w, 835 s, 690 w, 623 w cm^{-1}. UV–vis (hexane): 218, 244, 276 nm. EI MS (70 eV) *m/z*: 752, 624, 551, 377, 348. Anal. Calcd for $C_{18}H_{54}Si_8SnTe_2$: C, 24.87; H, 6.26. Found: C, 25.01; H, 6.23.

(67) Bonasia, P. B.; Seligson, A. L.; Arnold, J. Unpublished results.
(68) Gaffney, C.; Harrison, P. G.; King, T. J. *J. Chem. Soc., Chem. Commun.* **1980**, 1251.
(69) Cotton, J. D.; Cundy, C. S.; Harris, D. H.; Hudson, A.; Lappert, M. F.; Lednor, P. W. *J. Chem. Soc., Chem. Commun.* **1974**, 651.
(70) Hudson, A.; Lappert, M. F.; Lednor, P. W. *J. Chem. Soc., Dalton Trans.* **1976**, 2369.
(71) Gynane, M. J. S.; Harris, D. H.; Lappert, M. F.; Power, P. P.; Rivière, P.; Rivière-Baudet, M. *J. Chem. Soc., Dalton Trans.* **1977**, 2004.
(72) Schaeffer, C. D.; Myers, L. K.; Coley, S. M.; Otter, J. C.; Yoder, C. H. *J. Chem. Educ.* **1990**, *67*, 347.

Table VII. Conditions, Yields, and Product Analyses for Solution Thermolysis of $M[TeSi(SiMe_3)_3]_2$

		% yield[a]			wt %[c]			
compd	time (h)	MTe	$E[Si(SiMe_3)_3]_2$	total recovery	M[b]	Te[b]	C	H
1	229	22 (28)	69 (72)	91	40.3 (48.19)	34.7 (51.81)	0.46	0.03
2	22	32 (35)	63 (65)	95	58.3 (61.89)	39.8 (38.11)	0.56	0.14
4	96	28 (33)	56 (67)	84	71.4 (72.41)	28.2 (27.59)	1.23	0.28

[a] Theoretical yields in parentheses. [b] Calculated weight percentage for ME in parentheses. [c] Results from atomic adsorption and combustion analyses.

$Pb[TeSi(SiMe_3)_3]_2$ (2). A solution of $HTeSi(SiMe_3)_3$ (0.83 g, 2.2 mmol) in hexane (15 mL) at −78 °C was added to a solution of $Pb[N(SiMe_3)_2]_2$ (0.58 g, 1.1 mmol) at −78 °C in the same solvent (15 mL), resulting in the formation of a dark red solution. The reaction solution was stirred at this temperature for 30 min, the cold bath was removed, and the solution was stirred at room temperature for an additional 60 min. Workup as above, followed by crystallization from hexane (5 mL) at −40 °C for 24 h, yielded red crystalline **2** (0.86 g, 82%). Mp: 198–200 °C dec. ^1H NMR (400 MHz): δ 0.42 (s). $^{13}C\{^1H\}$ NMR (100 MHz): δ 2.41 (s). IR: 1244 m, 835 s, 743 w, 689 m, 622 m cm^{-1}. UV–vis (hexane): 218, 244, 276 nm. EI MS (70 eV) *m/z*: 624, 551, 377, 348. Anal. Calcd for $C_{18}H_{54}PbSi_8Te_2$: C, 22.57; H, 5.68. Found: C, 22.64; H, 5.63.

$Sn[SeSi(SiMe_3)_3]_2$ (3). $Sn[N(SiMe_3)_2]_2$ (0.59 g, 1.3 mmol) in hexane (10 mL) was combined with $HSeSi(SiMe_3)_3$ (0.88 g, 2.7 mmol) dissolved in hexane (10 mL) to give an orange solution. After 2 h of stirring, the solvent was removed under reduced pressure. The yellow-orange residue was extracted with hexane (40 mL), and the extract was filtered, concentrated, and cooled to −40 °C for several days. Yellow-orange crystals of **3** (0.88 g, 87%) were isolated by filtration. Mp: 209 °C dec. ^1H NMR (400 MHz): δ 0.44 (s). $^{13}C\{^1H\}$ NMR (100 MHz): δ 2.11 (s). IR: 1309 w, 1242 m, 835 s, 744 w, 688 m, 623 m cm^{-1}. UV–vis (hexane): 216, 232 nm. EI MS (70 eV) *m/z*: 722 (M^+), 574, 525, 348, 327. Anal. Calcd for $C_{18}H_{54}Se_2Si_8Sn$: C, 28.01; H, 7.05. Found: C, 28.16; H, 7.05.

$Pb[SeSi(SiMe_3)_3]_2$ (4). A solution of $HSeSi(SiMe_3)_3$ (0.66 g, 2.0 mmol) in hexane (15 mL) was added to a solution of $Pb[N(SiMe_3)_3]_2$ (0.54 g, 1.0 mmol) in the same solvent (10 mL), resulting in the formation of an orange solution. The mixture was stirred for 1.5 h and the solvent removed under reduced pressure. The dry residue was extracted with hexane (10 mL), and the solution was filtered, concentrated to 4 mL, and cooled to −40 °C for several days. Orange crystals of **4** (0.67 g, 76%) were isolated by filtration. Mp: 209–211 °C dec. ^1H NMR (400 MHz): δ 0.44 (s). $^{13}C\{^1H\}$ NMR (100 MHz): δ 2.07. IR: 1308 w, 1241 m, 859 s, 835 s, 744 s, 688 m, 623 m cm^{-1}. UV–vis (hexane): 220, 224, 286, 322, 418 nm. Anal. Calcd for $C_{18}H_{54}PbSe_2Si_8$: C, 25.13; H, 6.33. Found: C, 24.92; H, 6.50.

$Sn[SSi(SiMe_3)_3]_2$ (5). A solution of $HSSi(SiMe_3)_3$ (0.75 g, 2.6 mmol) in hexane (25 mL) was added to a solution of $Sn[N(SiMe_3)_2]_2$ (0.58 g, 1.3 mmol) in the same solvent (5 mL), resulting in the formation of an orange solution. The mixture was stirred for 2 h and the solvent removed under reduced pressure. The dry yellow-orange powder was extracted with hexane (10 mL), and the solution was filtered, concentrated to 3 mL, and cooled to −40 °C for several days. Yellow-orange crystals of **5** (0.56 g, 63%) were isolated by filtration. Mp: 222 °C dec. ^1H NMR (400 MHz): δ 0.44 (s). $^{13}C\{^1H\}$ NMR (100 MHz): δ 1.99 (s). IR: 1242 m, 835 s, 722 w, 688 m, 624 m cm^{-1}. UV–vis (hexane): 218, 384, 404 nm. EI MS (70 eV) *m/z*: 678 (M^+), 661, 637, 513, 485, 455. Anal. Calcd for $C_{18}H_{54}S_2Si_8Sn$: C, 31.88; H, 8.03. Found: C, 31.46; H, 7.80.

$Pb[SSi(SiMe_3)_3]_2$ (6). $Pb[N(SiMe_3)_2]_2$ (0.73 g, 14 mmol) in hexane (10 mL) was combined with $HSeSi(SiMe_3)_3$ (0.79 g, 2.8 mmol) dissolved in hexane (25 mL) to give an orange solution. After 2 h of stirring, the solvent was removed under reduced pressure. Extraction with hexane (20 mL) gave an orange solution that was filtered, concentrated, and cooled to −40 °C for several days. Orange crystals of **6** (0.67 g, 63%) were isolated by filtration. Mp: 239 °C dec. ^1H NMR (400 MHz): δ 0.43 (s). $^{13}C\{^1H\}$ NMR (100 MHz): δ 1.95 (s). IR: 1241 m, 835 s, 743 w, 688 m, 624 m cm^{-1}. UV–vis (hexane): 218, 238, 386 nm. Anal. Calcd for $C_{18}H_{54}S_2Si_8Pb$: C, 28.02; H, 7.10. Found: C, 27.82; H, 7.00.

$\{Sn[TeSi(SiMe_3)_3]_2\}_2$(dmpe) (7). A solution of **1** (0.69 g, 0.80 mmol) in hexane (10 mL) was layered with hexane (10 mL) followed by a solution of dmpe (0.13 mL, 0.80 mmol) in hexane (10 mL) in a 1-in. diameter Schlenk tube. After slow diffusion of the layers over several days at −40 °C, orange crystals of **7** (0.40 g, 75%) were isolated by filtration. Mp: 204–207 °C dec. ^1H NMR (400 MHz): δ 2.41 (s br, PCH_2, 4H), 1.32 (s br, PCH_3, 12H), 0.42 (s, $SiCH_3$, 108H). $^{13}C\{^1H\}$ NMR (100 MHz): δ 1.73 (s, $SiCH_3$). $^{31}P\{^1H\}$ NMR: δ −60.4 (s, $|J_{P^{117/119}Sn}|$ = 1555 Hz). $^{125}Te\{^1H\}$ NMR (toluene-d_8, −70 °C): δ −1175 (d, $|^2J_{TeP}|$ = 64 Hz). IR: 1282 w, 1255 w, 1240 m, 1106 w, 942 w, 898 w, 861 m, 834 s, 744 w cm^{-1}. FAB MS *m/z*: 1364, 869 $\{Sn[TeSi(SiMe_3)_3]_2\}$, 752 $\{[TeSi(SiMe_3)_3]_2\}$. Anal. Calcd for $C_{42}H_{124}P_2Si_{16}Sn_2Te_4$: C, 26.71; H, 6.62. Found: C, 26.61; H, 6.67.

$\{Sn[SeSi(SiMe_3)_3]_2\}_2$(dmpe) (8). A solution of **3** (0.34 g, 044 mmol) in hexane (10 mL) was layered with hexane (10 mL) followd by a solution of dmpe (0.07 mL, 0.44 mmol) in hexane (10 mL). The layers were allowed to diffuse slowly over 24 h at −40 °C. Pale yellow crystals of **8** (0.33 g, 75%) were isolated by filtration. Mp: 195 °C dec. ^1H NMR (400 MHz): δ 2.65 (s br, PCH_2, 4H), 1.23 (s br, PCH_3, 12H), 0.41 (s, $SiCH_3$, 108H). $^{13}C\{^1H\}$ NMR (100 MHz): δ 1.56 (s, $SiCH_3$). $^{31}P\{^1H\}$ NMR: δ −47.2 (s, $|J_{P^{117/119}Sn}|$ = 1525 Hz). IR: 1238 m, 1115 w, 949 w, 831 s, 687 w, 617 w cm^{-1}. Anal. Calcd for $C_{42}H_{124}P_2Si_{16}Sn_2Se_4$: C, 29.78; H, 7.38. Found: C, 29.97; H, 7.08.

$\{Sn[SSi(SiMe_3)_3]_2\}_2$(dmpe) (9). A solution of **5** (0.11 g, 0.16 mmol) in hexane (5 mL) was layered with hexane (5 mL) followed by a solution of dmpe (0.03 mL, 0.16 mmol) in hexane (5 mL). The layers were allowed to diffuse slowly over 24 h at −40 °C. Colorless crystals of **9** (0.08 g, 62%) were isolated by filtration. Mp: 247 °C dec. ^1H NMR (400 MHz): δ 2.65 (s br, PCH_2, 4H), 1.17 (s br, PCH_3, 12H), 0.40 (s, $SiCH_3$, 108H). $^{13}C\{^1H\}$ NMR (100 MHz): δ 1.40 (s, $SiCH_3$). $^{31}P\{^1H\}$ NMR: δ −35.4 (s, $|J_{P^{117/119}Sn}|$ = 1522 Hz). IR: 1284 2, 1241 m, 1116 w, 948 w, 908 w, 835 s, 743 w, 686 m, 624 m, 492 m cm^{-1}. Anal. Calcd for $C_{42}H_{124}P_2Si_{16}Sn_2S_4$: C, 33.49; H, 8.30. Found: C, 33.15; H, 8.11.

$(PMe_3)Sn[TeSi(SiMe_3)_3]_2$ (10). A solution of PMe_3 (0.031 mL, 0.30 mmol) in hexane (5 mL) was added to a solution of **1** (0.26 g, 0.30 mmol) in the same solvent (10 mL) to form a light orange solution. The solution was stirred for 0.5 h, and the solvent was removed under reduced pressure. The dry orange powder was extracted with hexane (10 mL), and the solution was filtered, concentrated to 3 mL, and cooled to −40 °C for 24 h. Orange crystals of **10** (0.23 g, 80%) were isolated by filtration. Mp: 142–143 °C dec. ^1H NMR (300 MHz): δ 1.09 (d, PCH_3, 9H), 0.43 (s, $SiCH_3$, 54H). $^{13}C\{^1H\}$ NMR (100 MHz): δ 1.98 (s, $SiCH_3$). $^{31}P\{^1H\}$ NMR: δ −78.9 (s, $|J_{P^{117/119}Sn}|$ = 1580 Hz). $^{125}Te\{^1H\}$ NMR (toluene-d_8, −40 °C): δ −1165 (d, $|J_{Te^{31}P}|$ = 79 Hz, $|J_{Te^{117/119}Sn}|$ = 1327 Hz). IR: 1280 w, 1239 m, 946 m, 834 m, 741 w, 688 m, 622 m cm^{-1}. Anal. Calcd for $C_{21}H_{63}PSi_8SnTe_2$: C, 26.80; H, 6.72. Found: C, 27.39; H, 6.55.

Generation of Other $(PR_3)Sn[TeSi(SiMe_3)_3]_2$ Complexes. To separate solutions of ca. 25 mg of **1** dissolved in C_6D_6 in an NMR tube was added 1 equiv of the phosphines PEt_3, PCy_3, PMe_2Ph, PPh_3, and $P(OMe)_3$. $^{31}P\{^1H\}$ NMR data for these complexes are given in Table IV.

Solid-State Pyrolysis of 1–6. A quartz crucible containing $M[ESi(SiMe_3)_3]_2$ (~25 mg) was positioned inside a Pyrex ampule that had been preheated to 250 °C under N_2 in a tube furnace. After several minutes, a waxy solid film began to collect on the cold walls of the ampule protruding from the furnace. The crucible was held at this temperature for 30 min, and then cooled to room temperature under a N_2 flow. The contents of the crucible were collected along with a sample of the waxy solid scraped from the ampule walls. These latter solids were determined to be the corresponding chalcogenides $E[Si(SiMe_3)_3]_2$ (E = Te, Se, S) by comparison of ^1H and $^{13}C\{^1H\}$ NMR spectra to those of authentic samples. Characterization data for the powder residues are given in Tables V and VI.

Solution Thermolysis of 1, 2, and 4. The compounds were dissolved in toluene (5 mL) in a glass ampule fitted with a Teflon stopcock. The stirred solution was heated at 100 °C in the dark for several hours to yield a dark solid; this was allowed to settle, and the yellow supernatant was removed by filtration. The solid was washed with hexane (2 × 5 mL) and dried under vacuum. Removal of the solvent from the filtrate gave a waxy solid that was determined to be $E[Si(SiMe_3)_3]_2$ (E = Te, Se) by comparison of ^1H and $^{13}C\{^1H\}$ NMR spectra to those of authentic samples. Further experimental details and characterization data are given in Tables VI and VII.

Solution Thermolysis of 3, 5, and 6. Approximately 25 mg of $M[ESi(SiMe_3)_3]_2$ was dissolved in benzene-d_6 (0.5 mL) in a Teflon-stoppered NMR tube. The solution was heated to 80 °C in the dark, and ^1H and $^{13}C\{^1H\}$ NMR spectra were recorded periodically. The results of these experiments are discussed in the text.

Solution Photolysis of 1 and 2. Approximately 25 mg of $M[E-Si(SiMe_3)_3]_2$ was dissolved in benzene-d_6 (0.5 mL) in a Teflon-stoppered NMR tube. The solution was photolyzed using a high-pressure 500-W Hg lamp for 12 h. The progress of the reaction was monitored periodically by ^1H and $^{13}C\{^1H\}$ NMR spectroscopy.

Reaction of 2 with CH_3CN. In an attempt to recrystallize **2** by layering a Et_2O solution of **2** on top of CH_3CN, a gray metallic precipitate was produced. This material was shown to be cubic PbTe by X-ray powder diffraction analysis. The yellow filtrate from the reaction was evaporated to dryness, and the waxy yellow-orange solid isolated was determined to be $Te[Si(SiMe_3)_3]_2$ by ^1H and $^{13}C\{^1H\}$ NMR spectroscopy.

Reaction of 2 with Pyridine. One equivalent of pyridine (2 μL, 0.02 mmol) was added to a benzene-d_6 solution of **2** (0.02 g, 0.02 mmol) in an NMR tube. After 24 h, a metallic precipitate was observed; $Te[Si(SiMe_3)_3]_2$ and pyridine were the sole products observed by ^1H and $^{13}C\{^1H\}$ NMR spectroscopy.

X-ray Structural Determinations. The structures were determined by Dr. F. J. Hollander at the UC Berkeley College of Chemistry X-ray facility, CHEXRAY.

1. Orange rectangular tablet-shaped crystals of **1** were obtained by slow crystallization from hexamethyldisiloxane at –40 °C. One of these crystals was mounted on a glass fiber using Paratone N hydrocarbon oil. The crystal was then transferred to an Enraf-Nonius CAD-4 diffractometer, centered in the beam, and cooled to –130 °C. Automatic peak search and indexing procedures yielded a monoclinic reduced primitive cell.

The 5784 raw intensity data were converted to structure factor amplitudes and their esd's by correction for scan speed, background, and Lorentz and polarization effects. Inspection of the azimuthal scan data showed a variation $I_{min}/I_{max} = 0.94$ for the average curve; an empirical correction based on the observed variation was applied to the data. Inspection of systematic absences indicated the possible space groups for **1** were $P2/c$ and Pc, and the successful solution and refinement of the structure in the centric group $P2/c$ confirmed this. Removal of the systematically absent data left 5171 unique data in the final data set.

The structure was solved by Patterson methods and refined via standard least-squares and Fourier techniques. In a difference Fourier map calculated following refinement of all non-hydrogen atoms with anisotropic thermal parameters, peaks were found corresponding to the positions of most hydrogen atoms. Hydrogen atoms were assigned idealized locations and values of B_{iso} approximately 1.2 times the B_{eqv} of the atoms to which they were attached. They were included in the structure factor calculations but not refined.

The final residuals for 262 variables refined against the 3502 data for which $F^2 > 3\sigma(F^2)$ were $R = 0.0373$, $R_w = 0.0385$, and GOF = 1.225. The R value for all 5171 data was 0.0702. The largest peak in the final difference Fourier map had an electron density of 1.31 e/Å^3, and the lowest excursion, –0.23 e/Å^3. The largest positive peaks were all located near the Sn and Te atoms.

10. Pale orange bladelike crystals were obtained by slow crystallization from hexanes at –40 °C. A crystal was mounted as above and cooled to –91 °C. Automatic peak search and indexing procedures yielded a triclinic reduced primitive cell. Inspection of the Niggli values revealed no conventional cell of higher symmetry.

The 5782 unique raw intensity data were converted to structure factor amplitudes and their esd's by correction for scan speed, background, and Lorentz and polarization effects. Inspection of intensity standards revealed a reduction of 22% of the original intensity; the data were corrected for this decay. Inspection of the azimuthal scan data showed a variation $I_{min}/I_{max} = 0.84$ for the average curve. However, the scans showed unacceptable differences between data points which should have been equivalent, indicating that the crystal orientation may have been compromised before scans were taken. An empirical correction was made to the data on the basis of the combined differences between F_o and F_c following refinement of all atoms with isotropic thermal parameters.[73] The choice of the centric group was confirmed by successful solution and refinement of the structure. The structure was solved by Patterson methods and refined via standard least-squares and Fourier techniques. Hydrogen atoms were assigned idealized locations and values of B_{iso} approximately 1.3 times the B_{eqv} of the atoms to which they were attached. They were included in structure factor calculations but not refined. In the final cycles of least-squares refinement, five data which appeared to be affected by multiple diffraction were given zero weight.

The final residuals for 298 variables refined against the 4927 accepted data for which $F^2 > 3\sigma(F^2)$ were $R = 0.0356$, $R_w = 0.0452$, and GOF = 1.73. The R value for all accepted data was 0.0438. The largest peak in the final difference Fourier map had an electron density of 1.01 e/Å^3, and the lowest excursion, –0.14 e/Å^3. All of the high-density peaks were located around the Te and Sn atoms.

Acknowledgment. Financial support from the National Science Foundation (Grant CHE-92-10406) is gratefully acknowledged.

Supplementary Material Available: Tables of temperature factor expressions, positional parameters, and intramolecular distances and angles (12 pages); listings of observed and calculated structure factors (65 pages). Ordering information is given on any current masthead page.

(73) Walker, N.; Stewart, D. *Acta Crystallogr.* **1983**, *A39*, 159.